

Emission Heights of Coronal Bright Points on Fe XII Radiance Map

H. Tian^a, C.-Y. Tu^{a,*}, J.-S. He^a, E. Marsch^b

^aDepartment of Geophysics, Peking University, Beijing 100871, China

^bMax-Planck-Institut für Sonnensystemforschung, 37191 Katlenburg-Lindau, Germany

Abstract

The study of coronal bright points (BPs) is important for understanding coronal heating and the origin of the solar wind. Previous studies indicated that coronal BPs have a highly significant tendency to coincide with magnetic neutral lines in the photosphere. Here we further studied the emission heights of the BPs above the photosphere in the bipolar magnetic loops that are apparently associated with them. As BPs are seen in projection against the disk their true emission heights are unknown. The correlation of the BP locations on the Fe XII radiance map from EIT with the magnetic field features (in particular neutral lines) was investigated in detail. The coronal magnetic field was determined by an extrapolation of the photospheric field (derived from 2-D magnetograms obtained from the Kitt Peak observatory) to different altitudes above the disk. It was found that most BPs sit on or near a photospheric neutral line, but that the emission occurs at a height of about 5 Mm. Some BPs, while being seen in projection, still seem to coincide with neutral lines, although their emission takes place at heights of more than 10 Mm. Such coincidences almost disappear for emissions above 20 Mm. We also projected the upper segments of the 3-D magnetic field lines above different heights, respectively, on to the tangent x-y plane, where x is in the east-west and y in the south-north direction. The shape of each BP was compared with the respective field-line segment nearby. This comparison suggests that most coronal BPs are actually located on the top of their associated magnetic loops. Finally, we calculated for each selected BP region the correlation coefficient between the Fe XII intensity enhancement and the horizontal component of the extrapolated magnetic field vector at the same x-y position in planes of different heights, respectively. We found that for almost all the BP regions we studied the correlation coefficient, with increasing height, increases to a maximal value and then decreases again. The height corresponding to this maximum was defined as the correlation height, which for most bright points was found to range below 20 Mm.

Key words: Coronal bright points; Magnetic loops; Correlation height

1. Introduction

Coronal bright points (BPs) were first observed in soft X-ray images (Vaiana et al., 1970), and later found to be also visible with enhanced intensity at EUV and radio wavelengths. This enhanced emission feature is 30''-40'' in size, often with a bright core of 5''-10'' (Madjarska et al., 2003). The lifetime of EUV bright point ranges from 5 hours to 40 hours, with an average of 20 hours (Zhang et al., 2001), while the average lifetime of an X-ray bright point is 8 hours as determined by Skylab X-ray observations (Golub et al., 1974). Brajša et al. (2004) used coronal BPs as tracers to analyze solar differential rotation, and concluded that the average height of BPs in different 10-degree-

latitude bins differs a lot (from about 5000 km to 22000 km), but on average is 8000 km to 12000 km above the photosphere.

Coronal bright points are associated with regions of mixed-polarity magnetic flux of the magnetic network (Webb et al., 1993; Falconer et al., 1998; Wilhelm et al., 2000; Xia et al., 2003). And most BPs are likely to be associated more with the cancellation of magnetic features than their emergence (Webb et al., 1993). Recent observations based on EIT/SOHO and TRACE confirmed that BP is strongly correlated with the evolution of the underlying bipolar magnetic region (Brown et al., 2001; Madjarska et al., 2003; Ugarte-Urra et al., 2004). Some BPs are observed to lie at the base of polar plumes in coronal holes and may eject mass into the solar wind (Ahmad & Webb, 1978). However, SUMER/SOHO observations indicated that BP regions correspond to no or

* Corresponding author.

Email address: chuanyitu@pku.edu.cn (C.-Y. Tu).

small outflow, and it was concluded that the fraction of the total mass flux contributed by BPs to the solar wind is negligible (Wilhelm et al., 2000; Madjarska et al., 2003; Xia et al., 2003). Spectroscopic analyses based on HRTS, SUMER, and CDS revealed the presence of small-scale transient brightenings within the bright point, but no relation was found between the bright point and the explosive events (Moses et al., 1994; Madjarska et al., 2003; Ugarte-Urra et al., 2004).

It was suggested that BPs may result from the interaction between two magnetic fragments with opposite polarities, which can lead to magnetic reconnection and local heating of the plasma (Priest et al., 1994; Parnell et al., 1994; Neukirch et al., 1997; Von Rekowski et al., 2006). The model proposed by Parnell et al. (1994) also suggested that BPs lie near the location where magnetic features cancel but not necessarily directly above it. Recently, Büchner et al. (2004a) and Büchner et al. (2004b) simulated the consequent formation of non-force-free current sheets in chromosphere and corona. Their model results suggest that the current sheets induced by photospheric motion supply the energy for the energization of BP.

The magnetic field used in the above cited observational analyses was the photospheric field. However, a BP is a EUV radiation phenomenon that occurs in the corona. So, a comparison should be made with the coronal magnetic field. Since the magnetic field above the photosphere can still not be obtained through direct observation, an extrapolation from a photospheric magnetogram is required, which will usually provide a good approximation to the real coronal field. For a review of this subject, see Wiegmann & Neukirch (2002).

In our present study we used the force-free-field extrapolation method proposed by Seehafer (1978) to extrapolate the field based on a Kitt Peak photospheric magnetogram to the corona. Then we combined this extrapolated magnetic field with the Fe XII radiance map from EIT, in order to study the relation of BPs with magnetic neutral lines and projections of magnetic loops. From these comparisons the height range of the BP locations could be roughly estimated.

2. Data analysis

We used a Fe XII (19.5 nm) filtergram from the observation that SOHO/EIT made at 19:13 UT on 16 March 1997. The pixel size of this coronal image is 2.6 seconds of arc, which is high enough to study coronal BPs. Our selected area of the image is a square centered on the solar disk, has a width of 0.6 solar radii and obviously does not include an active region. This area is shown in Figure 1 as a white rectangle.

The spatial filtering method described by Falconer et al. (2003) was used to produce the image of BPs. For the Fe XII intensity image, we chose two squares centered on each pixel, an outer square with a size of about two thirds of

a network cell (about 21000 km, or 11 pixels), and an inner square that was about one third of a network cell wide (about 9000 km, or 5 pixels). For each pixel, the background intensity was defined as follows: First the difference between the integrated intensities over the outer and inner square was calculated. Then this was divided by the difference between the areas of the two squares. The resulting ratio was defined as the background intensity in any given pixel, and hence we got a uniform background image. By subtracting this background image from the original one, we obtained an image of the intensity enhancement. Only contiguous sets of pixels in which the emission was enhanced by 30% or more above the local background were selected and defined as BPs, which are shown as dark patches in Figure 2. We also applied this method to the Fe XII filtergram that was observed six hours before, and thus found many BPs already existed at that time. In accordance to Zhang et al. (2001) who found lifetime of BPs ranges from 5 to 40 hours, this result revealed that coronal BPs are not simply transient events.

We used a Kitt Peak photospheric magnetogram that was obtained on the same day but about one and a half hours before the time of the EIT observation. This magnetogram has a pixel size of 1.15 seconds of arc and was summed over 2×2 pixels to reduce the noise level, as was discussed by Falconer et al. (1998). Both the magnetic field and EIT radiation were assumed to remain unchanged during this period. First the magnetogram was shifted to compensate for the solar rotation during the two observations. Then we did cross correlation between the EIT image and the magnetogram and obtained the optimal match of them. After that we chose the data of the magnetic field from the same area as the EIT image.

On the basis of the force-free-field assumption, Seehafer (1978) introduced a coronal magnetic field extrapolation technique which was applied to a finite rectangular segment of the solar atmosphere. The hypothesis of a force-free field generally can be applied at heights of about 400 km above the photosphere (Metcalf et al., 1995). This technique has been successfully used to describe the magnetic field in the transition region and lower corona in the papers by Tu et al. (2005a) and Tu et al. (2005b) for a quiet-sun region and coronal hole and by Marsch et al. (2006) for a polar coronal hole. By using this method, the 3-D magnetic field $\mathbf{B}(x, y, z)$ was extrapolated from the photosphere to the corona. This method is feasible because a coronal BP is a long-living feature, which lasts for more than several hours on an EIT image. In our study, the magnetic field was extrapolated from the photosphere to a height of 80 Mm. Then a 3×3 pixel boxcar smoothing function was applied to the absolute magnetic flux density at each height for which we made a data analysis. Those pixels that had a smoothed flux at the corresponding height below the noise level estimated by the method described below were masked out. We retained only the polarity data of the magnetic field in the unmasked pixels, which resulted in a distribution pattern of magnetic polarities. Figure 2 shows the distribution

pattern of magnetic polarities at 5 Mm (left panel) and 9 Mm (right panel). The regions with positive and negative magnetic flux density are outlined in blue and red, respectively. The estimated noise level at a height of h Mm, n_h , was derived from the following formula:

$$n_h = \frac{\overline{|B_{zh}|}}{\overline{|B_{z0}|}} n_0 \quad (1)$$

where $\overline{|B_{z0}|}$ and $\overline{|B_{zh}|}$ represent the mean values of the absolute magnetic flux density at the photosphere and the height of h in Mm, respectively, and n_0 is the noise level of the Kitt Peak photospheric magnetogram, which is assumed to be 3 Gauss, as discussed in Falconer et al. (1998). At the height of 5 Mm and 9 Mm, this value is 1.256 Gauss and 0.846 Gauss, respectively. In Figure 2, the two bright points edged by purple curves (around the coordinates of $(70'', 210'')$ in the left panel and $(-190'', -70'')$ in the right panel) will be used as examples for discussion. We define the direction in which the BP region has its largest extension as the preferred orientation. We can see that the preferred orientation of the first BP corresponds to a large angle (more than 60 degrees) with respect to the polarity-dividing neutral line. We name this a type I (perpendicular) BP. In contrast, the preferential orientation of the second variety, which we name type II (parallel) BP, is almost along the polarity-dividing line.

The real 3-D coronal magnetic field can be reconstructed or approximated by means of the extrapolated magnetic field. In order to find the relation between the locations of BPs and their supporting magnetic loops, we projected the upper segments of the 3-D magnetic field lines above different heights, respectively, onto the x-y tangent plane, where x is in the east-west direction and y is in the south-north direction. Figure 3 shows these projections at 5 Mm (left panel) and 9 Mm (right panel). The red lines represent closed field lines and the blue lines open field lines. The BP distribution pattern copied from Figure 2 was also redrawn at 5 Mm (left panel) and 9 Mm (right panel) for comparison.

3. Results and discussion

We found that, based on magnetic field extrapolation to the lower corona, most BPs are close to the neutral lines determined from mixed-polarity regions. This finding corroborates the long-known result that BPs are located close to neutral lines as identified from magnetic field observations in the photosphere. It is clearly seen in Figure 2 that in considerable number BPs appear above or close to neutral lines. For example, the BP around the coordinates $(70'', 210'')$ extends from about $200''$ to $230''$ in y direction. From the extrapolated magnetic field maps, both at 5 Mm and 9 Mm, we can see that a bright pattern crosses the nearby neutral line at about $217''$. For this case we conclude that the BP is located above a mixed-polarity region, or simply say neutral line. We examined all 22 BPs seen in Figure

2 with sizes larger than $10''$. We found that more than 14 BPs (64%) cover regions between different magnetic polarities based on the extrapolation to 5 Mm (see Figure 2, left panel). For the magnetic field extrapolated to 9 Mm (see Figure 2, right panel) we still found a considerable number of BPs (more than 10, corresponding to 46%) that are located above or near neutral lines. We continued this kind of comparison with the extrapolated field lines up to a height of 25 Mm. Our results show that some BPs still coincide with neutral lines based on extrapolation to more than 10 Mm. However, we cannot confirm such coincidence at heights above 20 Mm.

The spatial resolution in this analysis is limited by the low noise level of the available magnetic field data. The Kitt Peak magnetogram, which has a spatial resolution of $4.6''$ which is comparable with the data of EIT on SOHO, was the best one we could get with low noise level. Since the sizes of the BPs we analyzed in this work are all larger than $10''$, the major part of the BPs can be determined, and therefore our conclusion is believable to some extent. The correlation between the EIT intensity enhancement and the horizontal magnetic field component, and the non-correlation between the EIT intensity enhancement and the vertical magnetic field component, both give further support to the above conclusion (see Paragraph 4-7 in this section).

Figure 3 clearly reveals that nearly all BPs are located in regions with dense field-line concentrations corresponding to magnetic loops. Only a few BPs, especially the small ones, are overlaid on regions with sparse field lines or no loops. One possible reason may be that the pre-existent loops disappeared during the time interval between the acquisitions of the EIT coronal EUV image and the Kitt Peak magnetogram. Another possible reason is that some loops lower than 5 Mm or 9 Mm just cannot be shown and discriminated in projection on the images. However, the coincidence between the locations of magnetic loops and BPs is still very obvious. This relation suggests that the emission regions giving rise to most BPs are located on the top of coronal magnetic loops. From Figure 3 we can see the BPs have different shapes, which may mainly be divided into two types, such as type I (perpendicular) and type II (parallel) as defined in Section 2. For the type I BP region, like the one edged by a purple curve in Figure 2 (around the coordinate of $(70'', 210'')$ in the left panel), the projections of most overlying field lines are approximately oriented along the preferential direction. And for type II BP region, like the one edged by purple curve in Figure 2 (around the coordinate of $(-190'', -70'')$ in the right panel), most overlying loops are oriented across the preferential direction.

Then we rescaled the EIT image and the extrapolated magnetic field maps by means of interpolation, thus enforcing them to have the same pixel size of $1.15'' \times 1.15''$. In order to study the emission height of BPs, we calculated the correlation coefficients between the EIT Fe XII intensity enhancement and the horizontal component of magnetic field vector at different heights, respectively, for each BP. If it were located on the top of a loop, it should be

well correlated with the horizontal component of magnetic field. We found that the value of the correlation coefficient varied with increasing height. For almost all the BP regions analyzed, the correlation coefficient increases to a maximal value before it is decreasing again. The height related with this maximum was defined as correlation height.

Figure 4 shows two examples. For the edged bright point in Figure 2 (left panel), the correlation coefficients at different heights are shown in Figure 2 (left panel). We found that the correlation coefficient increases to a maximum of 0.65 at 5 Mm before decreasing above this height. The number of data points in this bright point region is 264, for which the critical correlation coefficient is 0.12 with 95% confidence. The horizontal bar shows a height range from 3.99 Mm to 7.85 Mm, in which the coefficient is above 95% of its maximum. Figure 4 (right panel) shows the curve of correlation coefficient for the edged bright point in Figure 2 (right panel). The number of data points for this calculation is 441, for which a critical value of 0.093 for the linear correlation coefficient is determined with 95% confidence. The maximum coefficient is 0.77 at 9 Mm, with a height range from 2.20 Mm to 14.11 Mm in which the coefficient is above 95% of its maximum.

For the different BPs, the height ranges obtained by this method are different. This indicates that BPs do generally not reside at the same height. Table 1 lists the correlation heights and height ranges for 10 large bright points (more than 200 data points, or with a size of larger than $16''$). We can conclude that the emission heights of most BPs are below 20 Mm. For all the selected BPs, the mean value of the correlation height with a standard error (the standard deviation divided by $\sqrt{10}$) is 10.2 ± 2.7 Mm. This result is largely consistent with that of Brajša et al. (2004), in which the calculated mean height of the point-like tracer subtype BP (the subsets of the other two subtypes of BPs were too small to get reliable results) is 11.6 ± 2.1 Mm, when using his interactive method.

We also evaluated the correlation between the Fe XII intensity enhancement and the vertical magnetic field at different heights, respectively, for each selected BP. In this case, however, no obvious correlation was found. This fact proves further that the emission regions giving rise to most BPs are located on the top of coronal magnetic loops, where the magnetic field is horizontal. This picture is consistent with the result of the model suggested by Büchner et al. (2004a) and Büchner et al. (2004b), which implies that the plasma flow in the photosphere causes the formation of a localized current sheet in and above the transition region at the position of the EUV BP, and the dissipation in the current sheet supplies energy to the BP. Some authors suggested that flares, coronal heating, and spicules are driven by the same process such as core-field explosion (Falconer et al., 1998; Moore et al., 1999). If this picture reflects reality, one would naturally propose that BPs, being indicators of local coronal heating, can be produced by the same process leading to flares. The idea that most BP emission is limited to the loop top is consistent with the obser-

vation that hard X-ray emission is often seen at the top of large flaring loops (Masuda et al., 1994). It is possible that there exists, around the loop top, inverted Y-shaped field lines, like those proposed in Masuda et al. (1994), and that reconnection intermittently takes place, thus leading to a bright point. However, there may be other processes besides reconnection accounting for the result that the emission in the Fe XII channel of EIT is limited to the loop apex. If it is not reconnection at the loop top leading to the BP, then one has to heat up the entire loop and fill it with hot dense plasma. If then the emission in the Fe XII channel of EIT is limited to the loop top, this would imply that the top of the loop supporting a BP has the highest temperature.

It should be pointed out that our results may not be fully conclusive. Several factors can influence these results. First, the boundaries of BPs depend on the method we used for identifying the BPs as described in Section 2. Second, we assumed that the intensity of BPs and the magnetic field did not change a lot during the time span between the observations of EIT and Kitt Peak, which is about one and a half hours. Third, we only apply the correlation method to BPs with a large size (larger than $16''$). The pixel size of the final 2-D extrapolated magnetic field map is $2.88''$. To get a sufficiently large number of data points, we can only apply the correlation method to the relatively large bright points. This limitation may be overcome only in future higher-resolution studies.

4. Summary

We constructed the coronal magnetic field at different heights above the photosphere by extrapolating photospheric magnetograms obtained at the Kitt Peak solar observatory. From this data we obtained the magnetic vector field and polarity distribution at different heights. By a comparison of these patterns with an EIT image of Fe XII coronal bright points, we found that the coincidence of neutral lines and bright points at a height of about 5 Mm is highly significant. And this feature remains still obvious up to more than 10 Mm for some bright points. Above 20 Mm, there is no clear coincidence between bright points and neutral lines.

By comparing the projections of the upper segments of the 3-D magnetic field lines above different heights on to the tangent x-y plane with the image of the Fe XII coronal bright points, we come to the conclusion that a bright point is an emission region located around the apex of the associated magnetic loop.

From correlations between the horizontal component of the magnetic field vector at different heights and the square root of the Fe XII intensity enhancement in some large bright point regions, we derived a rough height range for the possible location of each bright point. For almost all the bright point regions analyzed, we find that with increasing height the correlation coefficient increases to a maximum and then decreases again. The corresponding height is de-

fined as correlation height, which is found to be smaller than 20 Mm for most of the bright points. For each selected bright point, we also obtained a height range in which the coefficient is above 95% of its maximum. We think the source of the bright-point emission is probably confined within this height range. Our results indicate that for most bright points the emission occurs below 20 Mm.

Acknowledgments

This work was supported by the National Natural Science Foundation of China under contracts 40574078, 40336053 and 40436015. It was also supported by the Beijing Education Project XK100010404. We thank the SOHO/EIT experiment team for providing the coronal images. We also thank the NSO/Kitt Peak observatory for the use of their magnetic field data.

References

- Ahmad, I. A., and Webb, D. F., X-ray analysis of a polar plume, *Sol. Phys.*, 58, 323, 1978.
- Brajša, R., Wöhl, H., Vršnak, B., Ruždjak, V., Clette, F., Hochedez, J.-F., and Roša, D., Height correction in the measurement of solar differential rotation determined by coronal bright points, *A&A*, 414, 707, 2004.
- Brown, D. S., Parnell, C. E., DeLuca, E. E., Golub L., and McMullen, R. A., The magnetic structure of a coronal X-ray bright points, *Sol. Phys.*, 201, 305, 2001.
- Büchner, J., Nikutowski, B., and Otto, A., Coronal heating by transition region reconnection, J. and Walsh, R. (eds.), *Coronal Heating, Proceedings of the SOHO-15*, Vol. ESA SP-575, 2004a.
- Büchner, J., Nikutowski, B., and Otto, A., Magnetic coupling of photosphere and corona: MHD simulation for multi-wavelength observations, Stepanov, A., Benevolenskaya, E. and Kosovichev, A. (eds.), *Multi-Wavelength Investigations of Solar Activity, Proceedings of the IAU Symposium*, Vol. 223., 2004b.
- Falconer, D. A., Moore, R. L., Porter, J. G., and Hathaway, D. H., Network coronal bright points: coronal heating concentrations found in the solar magnetic network, *ApJ*, 501, 386, 1998.
- Falconer, D. A., Moore, R. L., Porter, J. G., and Hathaway, D. H., Solar coronal heating and the magnetic flux content of the network, *ApJ*, 593, 549, 2003.
- Golub, L., Krieger, A. S., Silk, J. K., Timothy, A. F., and Vaiana, G. S., Solar X-Ray Bright Points, *ApJ*, 189, L93, 1974.
- Madjarska, M. S., Doyle, J. G., Teriaca, L., and Banerjee, D., An EUV Bright Point as seen by SUMER, CDS, MDI and EIT on-board SoHO, *A&A*, 398, 775, 2003.
- Marsch, E., Zhou, G.-Q., He, J.-S. and Tu, C.-Y., Magnetic structure of the solar transition region as observed in various ultraviolet lines emitted at different temperatures, *A&A*, 457, 699, 2006.
- Masuda, S., Kosugi, T., Tsuneta, S., Hara, H., Ogawara, Y., Loop-top hard X-ray source in a compact solar flare as evidence for magnetic reconnection, *Nature*, 371, 495, 1994.
- Metcalf, T. R., Jiao, L., McClymont, A. N., Canfield, R. C., Is the solar chromospheric magnetic field force-free? *ApJ*, 439, 474, 1995.
- Moore, R. L., Falconer, D. A., Porter, J. G., and Suess, S. T., On heating the Sun's corona by magnetic explosions: Feasibility in active regions and prospects for quiet regions and coronal holes, *ApJ*, 526, 505, 1999.
- Moses, D., Cook, J. W., Bartoe, J.-D. F., et al., Solar fine scale structures in the corona, transition region, and lower atmosphere, *ApJ*, 430, 913, 1994.
- Neukirch, N., Dreher, J., and Birk, G. T., Three dimensional simulation studies on bright points in the solar corona, *Adv. Space Res.*, 19, 1861, 1997.
- Parnell, C. E., Priest, Eric R., Titov, V. S., A model for X-ray bright points due to unequal cancelling flux sources, *Sol. Phys.*, 153, 217, 1994.
- Priest, E. R., Parnell, C. E., Martin, S. F., A converging flux model of an X-ray bright point and an associated canceling magnetic feature, *ApJ*, 427, 459, 1994.
- Seehafer, N., Determination of constant force-free solar magnetic fields from magnetograph data, *Sol. Phys.*, 58, 215, 1978.
- Tu, C.-Y., Zhou, C., Marsch, E., Wilhelm, K., Zhao, L., Xia, L.-D., and Wang, J.-X., Correlation heights of the sources of solar ultraviolet emission lines, *ApJ*, 624, L133, 2005a.
- Tu, C.-Y., Zhou, C., Marsch, E., Xia, L.-D., Zhao, L., Wang, J.-X., and Wilhelm, K., Solar Wind origin in Coronal Funnels, *Science*, 308, 519, 2005b.
- Ugarte-Urra, I., Doyle, J. G., Madjarska, M. S., and O'Shea, E., Signature of oscillations in coronal bright points, *A&A*, 418, 313, 2004.
- Vaiana, G. S., Krieger, A. S., Van Speybroeck, L. P., and Zehnpfennig, T., *Bull. Am. Phys. Soc.*, 15, 611, 1970.
- Von Rekowski B., Parnell, C. E., Priest, E. R., Solar coronal heating by magnetic cancellation - I. Connection equal bipoles, *Monthly notices of the royal astronomical society*, 366, 125, 2006.
- Webb, D. F., Martin, S. F., Moses, D., and Harvey, J. W., The correspondence between x-ray bright points and evolving magnetic features in the quiet sun, *Sol. Phys.*, 144, 15, 1993.
- Wiegelmann, T. and Neukirch, T., Including stereoscopic information in the reconstruction of coronal magnetic fields, *Sol. Phys.*, 208, 233, 2002.
- Wilhelm, K., Dammasch, I. E., Marsch, E., Hassler, D. M., On the source regions of the fast solar wind in polar coronal holes, *A&A*, 353749, 2000.
- Xia, L. D., Marsch, E. and Curdt, W., On the outflow in an equatorial coronal hole, *A&A*, 399, L5, 2003.
- Zhang, J., Kundu, M. R., and White, S. M., Spatial distri-

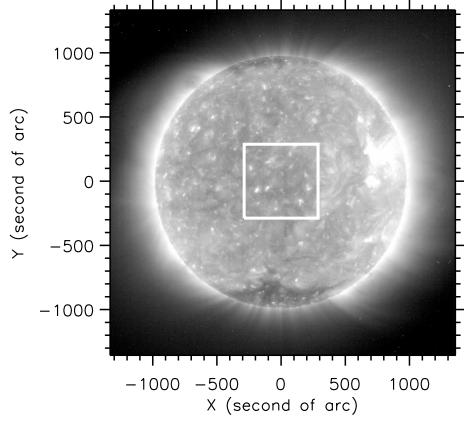


Fig. 1. Fe XII (19.5 nm) intensity image from an observation made by SOHO/EIT at 19:13 UT on 16 March 1997. The white square with a width of 0.6 solar radii on the disk center is the area which we chose for our study.

tribution and temporal evolution of coronal bright points,
Sol. Phys., 198, 347, 2001.

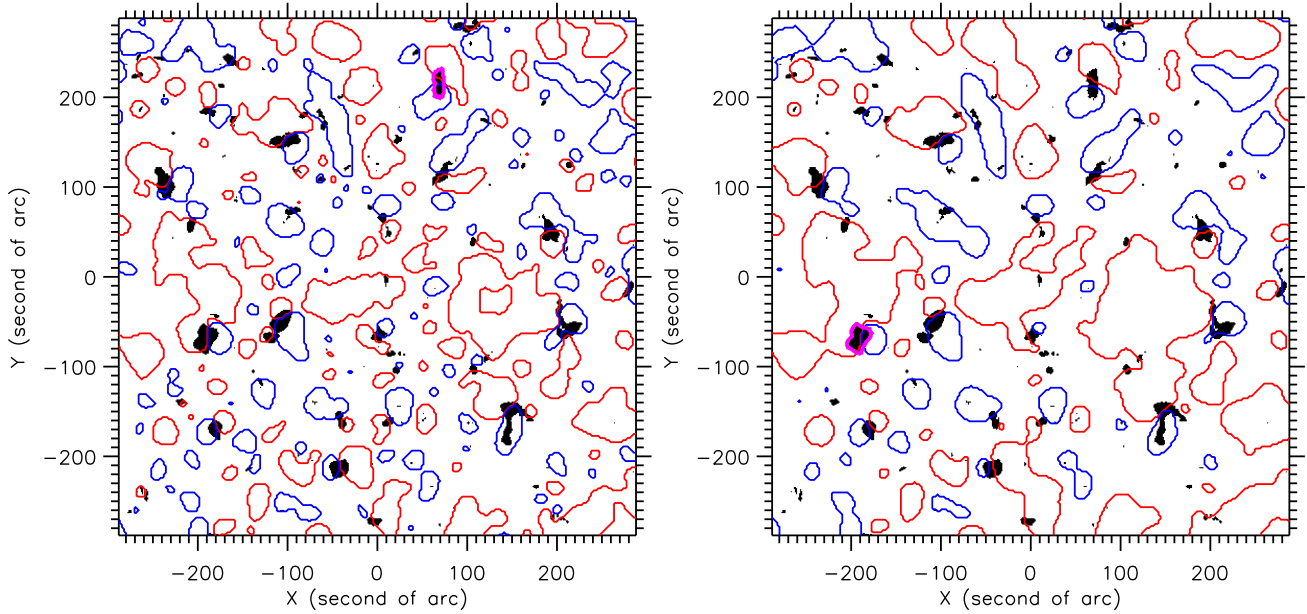


Fig. 2. The EIT coronal bright points registered are shown on the map of magnetic polarities at 5 Mm (left panel) and 9 Mm (right panel). The dark regions represent EIT BPs, the emission of which was enhanced by more than 30% above the background. Regions with positive and negative magnetic flux density are outlined in blue and red color, respectively. The two BPs edged by purple curves (around the coordinates of $(70'', 210'')$ in the left panel and $(-190'', -70'')$ in the right panel) are used as examples for the discussion in the text.

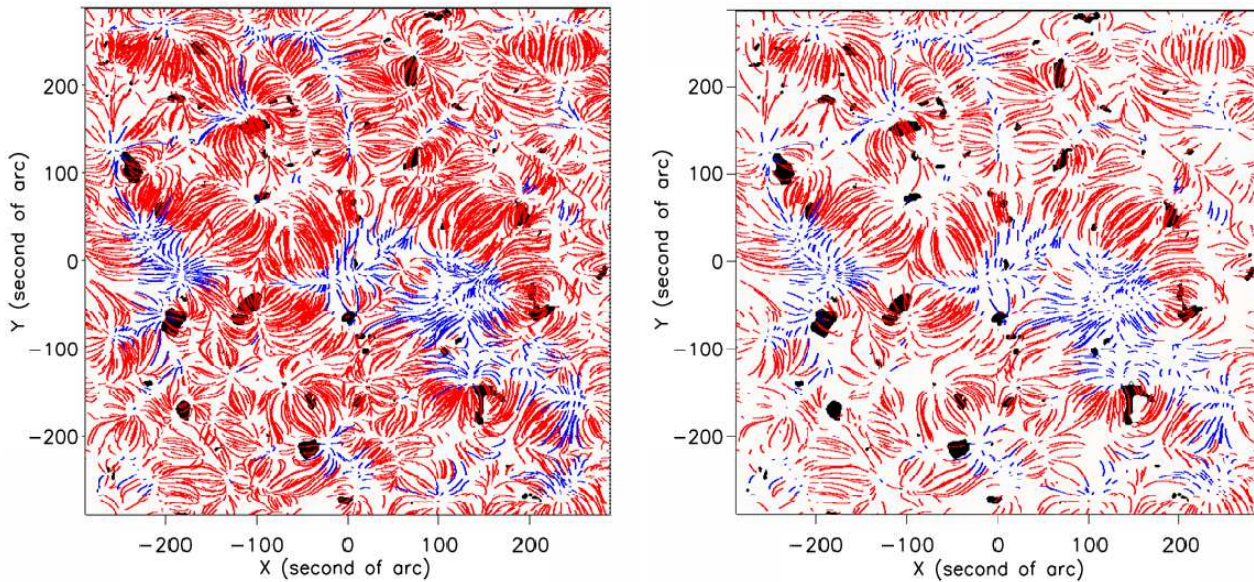


Fig. 3. Projections of the upper segments of the 3-D magnetic field lines above 5 Mm (left panel) and 9 Mm (right panel) on the x-y plane. The red lines represent closed field lines, and the blue lines correspond to open field lines. Dark regions indicate BPs, which are the same ones as already shown in Figure 2.

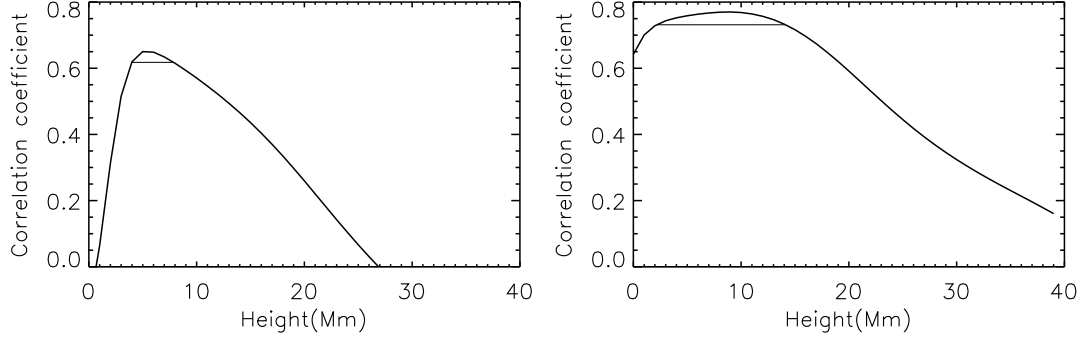


Fig. 4. Correlation coefficient between the horizontal component of magnetic field and the square root of the Fe XII intensity enhancement for the two color-edged BPs shown in Figure 2. For the first BP (left panel), the maximum correlation coefficient is 0.65 at 5 Mm. The horizontal bar shows the height range, from 3.99 Mm to 7.85 Mm, in which the coefficient is above 95% of its maximum. For the second BP (right panel), the maximum coefficient is 0.77 at 9 Mm. In the height range from 2.20 Mm to 14.11 Mm the coefficient is above 95% of its maximum.

Table 1
Correlation heights and height ranges of some bright points

Bright point	Number of data points in the bright point region	Maximum correlation coefficient	Critical correlation coefficient with 95% confidence	Correlation height (Mm)	Height range in which the coefficient is above 95% of its maximum (Mm)
1	264	0.65	0.120	5	3.99-7.85
2	441	0.77	0.093	9	2.20-14.11
3	263	0.61	0.120	13	5.56-16.46
4	310	0.49	0.111	24	20.32-31.00
5	262	0.39	0.120	1	0.19-1.47
6	489	0.72	0.088	11	5.91-19.21
7	283	0.31	0.116	1	0-1.03
8	205	0.47	0.136	25	22.59-29.08
9	434	0.73	0.094	3	0.77-14.92
10	371	0.55	0.101	10	6.30-13.73